Journal of Advanced Scientific Research

Available online through https://sciensage.info

ISSN 0976-9595

Research Article

A COMPREHENSIVE ELECTRONIC, VIBRATIONAL, NATURAL BOND ORBITAL AND REACTIVITY DESCRIPTOR ANALYSIS OF PHARMACOLOGICALLY IMPORTANT MOLECULE MIGALASTAT: A THEORETICAL STUDY

Abhishek Khare[1], Vijay Narayan[2], Ashok Kumar Singh[3], Amarendra Kumar*[1]

[1]*Department of Physics, University of Lucknow, Uttar Pradesh, India*

[2]*Department of Physics, SRMGPC, Lucknow, India*

[3]*Department of Chemistry, University of Lucknow, Uttar Pradesh, India*

**Corresponding author: akgkp25@yahoo.co.in*

Received: 08-10-2021; Revised: 27-02-2022; Accepted: 05-03-2022; Published: 31-03-2022

 https://doi.org/10.55218/JASR.202213222

ABSTRACT

Migalastat (Galafold) is a pharmacological chaperone indicated for the long term treatment for fabry disease a rare genetic disorder in adults. Quantum chemical calculations of energy, geometrical shape and vibrational wavenumbers of Migalastat have been accomplished by the usage of DFT method. The specific exploration of the infrared spectra of the compound underneath have a look at is centered on potential energy distribution (PED). Dipole moment, polarizability and first order static hyperpolarizability calculation using DFT/B3LYP/6-311G(d,p) level of theory outlined the nonlinear optical behavior of the underlying molecule. The frontier molecular orbitals and molecular electrostatic potential map were additionally given to clarify the molecular characteristics of the compound. To show the chemical activity of the chemical compound, reactivity descriptors and thermodynamic properties were also calculated utilizing 6-311G(d,p) basis set. Electron density distribution on atoms and bonds of given molecule was interpreted by its complete NBO analysis.

Keywords: Frontier orbital, NLO, NBO, Fukui function, First order hyperpolarizibility.

1. INTRODUCTION

In Molecular biology, misfolding of protein can cause severe damage even deleterious to cells function because of protein misrouting within the cells. To correct such misfolding, we need pharmacological chaperone which re-route proteins within cells [1]. A pharmacological chaperone can help improve the gastrointestinal symptoms and reduce the left ventricular mass in patients with Fabry disease. In addition, it can trigger a reduction in the kidney substrate clearance and improve the overall health of these individuals [2-4]. Migalastat is a pharmacological chaperone that binds preferentially and reversibly to the active sites of specific mutant kinds of alpha-galactosidase (amenable GLA mutations) [5, 6]. The purpose of this paper is to look into the structural, electrical, and vibrational properties of Migalastat. At the DFT level, the structure and harmonic wavenumbers were calculated and studied using the premise set 6-311G (d,p). Migalastat's optimal shape and molecular attributes including ground energy, FMO gap, molecular electrostatic potential, dipole moment, polarizability, and initial static hyperpolarizability have all been discussed elaborately. An entire vibrational analysis of the molecule has been finished with the aid of the quantum chemical calculations [7, 8]. As evidenced by studies conducted by various groups, computations based on DFT contribute to an additional explanation of vibrational spectroscopy data by providing not only qualitative but also quantitative information of each modes of vibration on the concept of PED [9-11].

2. COMPUTATIONAL DETAILS

All computation were done on PC utilizing blend of DFT/B3LYP strategy and 6-311G(d, p) basis set. The Gaussian 03 programme set [12], which involves gradient-optimized geometry [13], is a collection of programmes. For the computation of molecular shape, vibrational frequencies, FMO, and energies of

optimal shape, the DFT with the 3-parameter hybrid functional (B3) for the exchange part and the Lee-Yang-Parr (LYP) correlation function [14-16] was used. The software Gauss View 3.0 [17] was used to create visual graphics as well as to describe normal modes. The geometry to be put on the PES at the genuine local minima was confirmed by positive data of all computed wavenumbers. A uniform scaling component of 0.9679 [18, 19] has been included because the DFT/B3LYP functional appears to overstate the normal vibration modes. Combining the findings of the Gauss view software and the VEDA 4 application [20], the vibrational wavenumber assessments have been accomplished. The polarizability, static hyperpolarizability and dipole moment have also been evaluated employing DFT and are measured using Buckingham's definitions [21].

$$\mu = (\mu_x^2 + \mu_y^2 + \mu_z^2)^{1/2}$$

$$<\alpha> = 1/3\,[\,\alpha_{xx} + \alpha_{yy} + \alpha_{zz}]$$

The total intrinsic hyperpolarizability β_{TOTAL} [22] is specified as

$$\beta_{TOTAL} = [\beta_x^2 + \beta_y^2 + \beta_z^2]^{1/2}$$

Where $\beta_x = \beta_{xxx} + \beta_{xyy} + \beta_{xzz}$, $\beta_y = \beta_{yyy} + \beta_{yzz} + \beta_{yxx}$, $\beta_z = \beta_{zzz} + \beta_{zxx} + \beta_{zyy}$.

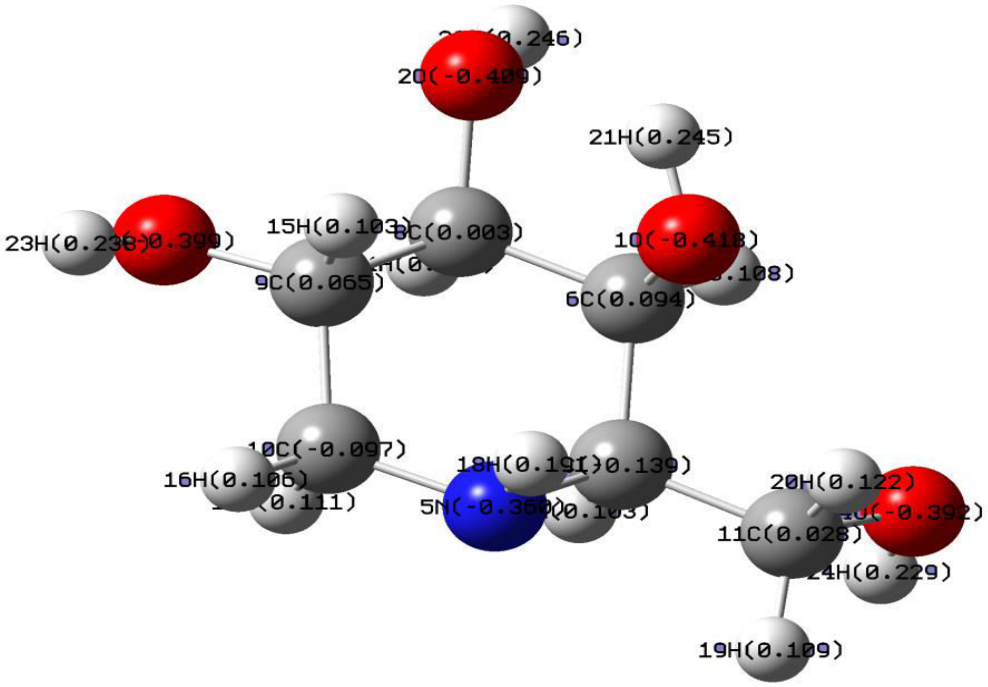

Fig. 1: Optimized Structure of Migalastat

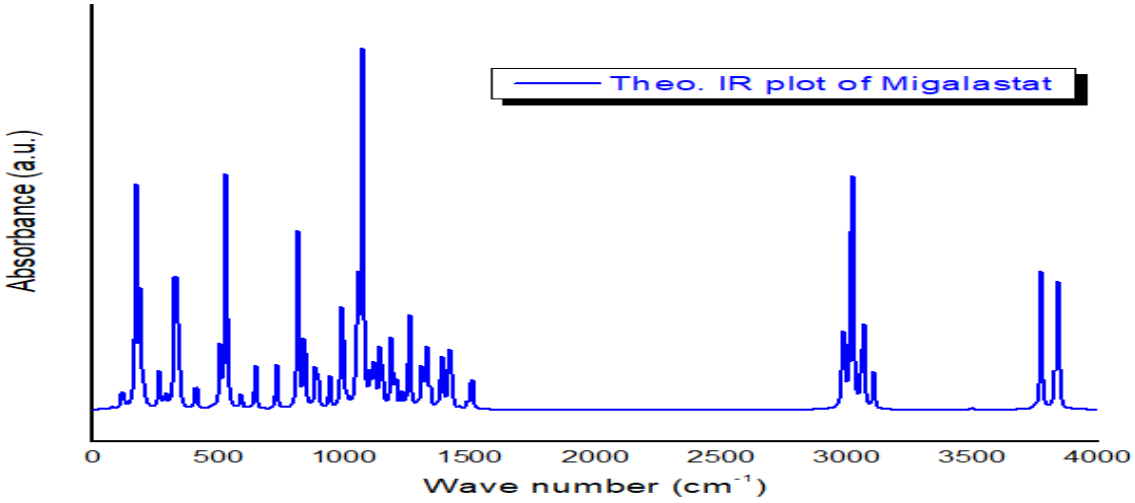

Fig. 2: Theoretical IR Plot of Migalastat

3. RESULT AND DISCUSSION

3.1. Molecular geometry

The optimal shape of Migalastat has been given in Fig.1. The molecule's geometry was optimized via minimizing energy employing DFT/B3LYP with the basis set 6-311G (d,p). Because there is no unreal frequency in the vibrational spectra, the optimal form of the chemical under attention is tested to be placed on the local genuine minima at the PES. The optimized structural parameters of the identify compound at the same level of theory are listed in Table1.

The bond length of C-H varies between 1.09Å and 1.54 Å, while the bond size of C-C ranges in 1.52 Å and 1.53 Å. Whereas the bond length of C-O for the molecule vary within the range of 1.42Å-1.43Å. The bond length of C-N is 1.46Å. The bond angle between C7-C6-C8 and C6-C8-C9 are found to be 111.4603° and 112. 0959° while angle between C7-N5-C10 is 110.9954°.

Table 1: Optimized Parameter of Migalastat computed at B3LYP/6-311 G(d,p) level

Parameter	Theoretical	Parameter	Theoretical	Parameter	Theoretical
Bond length		C11-O4-H24	107.7711	**Dihedral**	
O1-C6	1.4267	C7-N5-C10	110.9954	N5-C10-H16	109.0773
O1-H21	0.9664	C7-N5-H18	107.8499	N5-C10-H17	108.6813
O2-C8	1.4372	C10-N5-H18	109.1545	C9-C10-H16	109.3062
O2-H22	0.9617	O1-C6-C7	107.5285	C9-C10-H17	107.796
O3-C9	1.4275	O1-C6-C8	109.0716	H16-C10-H17	106.7181
O3-H23	0.9614	O1-C6-H12	110.0678	O4-C11-C7	112.2186
O4-C11	1.4256	C7-C6-C8	111.4603	O4-C11-H19	111.9381
O4-H24	0.9621	C7-C6-H12	109.2507	O4-C11-H20	105.8634
N5-C7	1.4647	C8-C6-H12	109.4393	C7-C11-H19	108.5553
N5-C10	1.4627	N5-C7-C6	111.8698	C7-C11-H20	109.6545
N5-H18	1.0172	N5-C7-H11	110.303	H19-C11-H20	108.5174
C6-C7	1.5342	N5-C7-H13	106.9931		
C6-C8	1.5374	C6-C7-H11	112.1866		
C6-H12	1.0993	C6-C7-H13	107.5944		
C7-C11	1.5326	H11-C7-H13	107.6255		
C7-H13	1.1003	O2-C8-C6	108.7661		
C8-C9	1.5252	O2-C8-C9	107.5411		
C8-H14	1.0976	O2-C8-H14	110.4555		
C8-H14	1.5438	C6-C8-C9	112.0959		
C9-H15	1.0974	C6-C8-N14	110.1003		
C10-H16	1.0948	C9-C8-H14	107.8541		
C10-H17	1.0962	O3-C9-C8	107.2468		
C11-H19	1.0962	O3-C9-H10	110.6747		
C11-H20	1.0911	O3-C9-H15	110.5739		
Bond Angle		C8-C9-H10	111.2079		
C6-O1-H21	105.5075	C8-C9-H15	107.435		
C8-O2-H22	108.4715	C10-C9-H15	109.6334		
C9-O3-H23	108.2286	N5-C10-C9	114.9438		

3.2. Electronic properties

The frontier orbitals, decide the manner in which a compound interacts with other compound. It's difference helps to describe the molecule's reactivity and stability. A low band gap makes a molecule more polarizable and is commonly related to excessive bioactivity and low stability [23].

In our study, band gap is measured to be 6.827eV. The three dimensional plots of the atomic frontier orbitals and the MESP map for Migalastat is presented in Fig.3 and Fig.4 respectively.

Fig. 3 shows that highest occupied molecular orbital is almost uniformly dispersed around the aromatic heterocyclic ring and has strong anti-bonding

belongings. The lowest unoccupied molecular orbital is discovered to be distributed throughout the alcohol group.

The MESP shown for Migalastat jointly depicts molecule form, size, and electrostatic potential values. MESP mapping is extremely vital in evaluating the molecular structure and its physical and chemical properties correlations [24-30]. It can be seen from right side of Fig. 4 that the Migalastat's MESP clearly depicts the five primary negative potential zones, which are distinguished by colour yellowish red across the four oxygen and nitrogen atoms, whilst the Hatoms of the heterocyclic ring have a positive potential (green). The MESP has been employed to outline the intra-charge transfer path. As indicated on the left side of Fig. 4, we plotted Migalastat electrostatic potential contour plots. Electric field line is concentric along the oxygen atom in the 2D plot, indicating that oxygen of O-H functions as a negative charge centre.

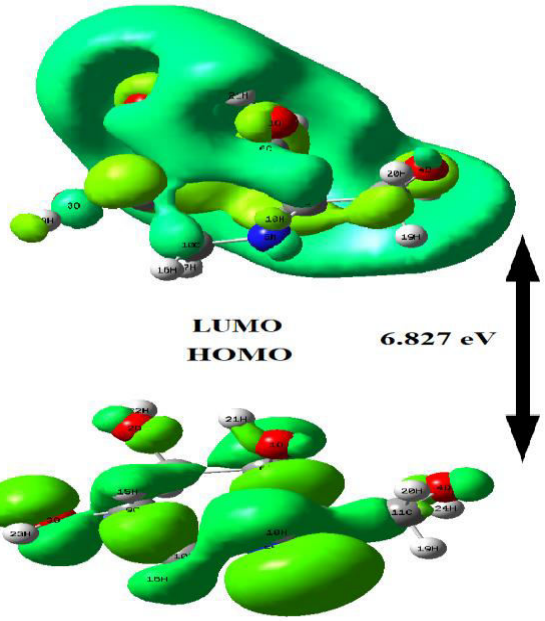

Fig. 3: HOMO LUMO Plot of Migalastat

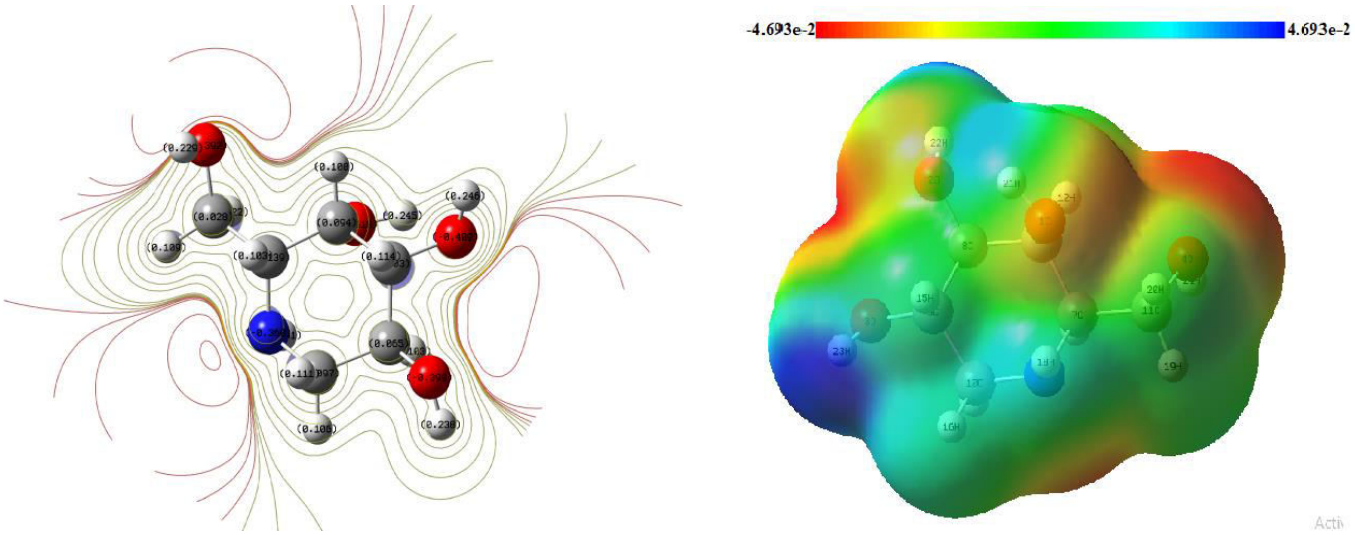

Fig. 4: Contour plot and MEP surface for Migalastat

3.3. Vibrational assessment

The optimal molecular shape of Migalastat corresponds to the C1 point group because it lacks any special symmetry. A total no. of 66 (3N-6) ways of vibrations possible having 24 atoms, which have been elaborated and given schematic abbreviations for vibrations such as stretching (symmetric and asymmetric), bending (in and out), torsion in the Table 2. It is widely understood that the vibrational wavenumbers are routinely overestimated by *ab-initio* and DFT methods. These inconsistencies can be fixed by explicitly estimating anharmonic correlations, introducing a scaled field [31], or directly scaling the estimated wavenumbers with an appropriate factor of 0.9679 [32].

3.3.1. O-H vibrations

The stretching of oxygen hydrogen (O-H) is very receptive to hydrogen bonding. A free hydroxyl group or a non-hydrogen bound hydroxyl group absorbs in the 3700-3500 cm^{-1} range. The system's intramolecular hydrogen bonding decreases the hydroxyl stretching band to the 3559-3200 cm^{-1} [33]. The scaled wavenumber calculated at 3719 cm^{-1}, 3718 cm^{-1}, 3704 cm^{-1} and 3647 cm^{-1} in the case of Migalstat are identified as O-H stretching with 100% contribution to P.E.D.

Table 2: Vibrational wavenumbers assessment of Migalastat

Unscaled frequency (cm^{-1})	Scaled frequency (cm^{-1})	Assignment
3842	3719	ν (O3-H23)100
3841	3718	ν (O2-H22)100
3827	3704	ν (O4-H24)100
3768	3647	ν(O1-H21)100
3494	3382	ν (N5-H18)100
3105	3005	ν (C11-H20)91
3062	2964	ν_{as}(C10-H17)34+ ν (C10-H16)60
3024	2927	ν_{as}(C8-H14)33 + ν (C9-H15)13+ ν_{as} (C10-H16)25 + ν_{as} (C10-H17)22
3019	2922	ν (C11-H19)90
3016	2919	ν_{as} (C8-H14)33 + ν (C10-H17)43
3006	2909	ν(C8-H14)18+ ν (C9-H15)72
2988	2892	ν (C6-H12)61+ ν (C7-H13)29
2978	2882	ν_{as} (C6-H12)23+ ν (C7-H13)71
1511	1462	β (H20-C11-H19)62 + τ_{out} (H20-C11-C7-C6)20
1508	1459	β (H18-N5-C10)52 + τ_{out}(H18-N5-C10-C9)13
1490	1442	β (H17-C10-H16)73
1459	1412	ν (C9-C8)13
1422	1376	β_{out} (H21-O1-C6)26
1420	1374	β (H24-O4-C11)16 + β(H20-C11-H19)25 + τ(H20-C11-C7-C6)35
1397	1352	β_{out} (H14-C8-O2)11
1392	1347	β_{out} (H24-O4-C11)25+ τ_{out} (H13-C7-N5-C10)25
1388	1343	ν (C6-C7)21
1368	1324	τ (H17-C10-N5-C7)19
1343	1300	β_{out} (H13-C7-N5)20 + β(H16-C10-N5)22
1340	1297	β(H15-C9-O3)15
1327	1284	ν_{as} (C8-C6)11
1315	1273	β(H14-C8-O2)17
1306	1264	β (H22-O2-C8)13
1262	1221	τ_{out} (O1-C7-C8-C6)16
1231	1191	β (H21-O1-C6)22
1205	1166	β (H23-O3-C9)15
1186	1148	β (H14-C8-O2)13
1146	1109	ν_{as} (N5-C10)12
1124	1088	ν_{as} (N5-C7)17 + ν(N5-C10)26
1107	1071	β (H24-O4-C11)11
1101	1066	ν (O3-C9)15+ ν (O4-C11)19
1073	1038	ν (O3-C9)45+ ν_{as} (O4-C11)16
1071	1037	ν (C9-C8)29
1055	1021	ν (O4-C11)16+ ν (O2-C8)30
1046	1012	ν (O4-C11)22
1001	969	ν (O2-C8)24
991	959	ν (O1-C6)18+τ (H19-C11-C7-C6)12
942	912	ν (C8-C6)12
891	862	ν (C6-C7)25
844	817	τ (H18-N5-C10-C9)25
816	790	ν (N5-C7)18
735	711	β_{out} (C6-C7-N5)13 + τ_{out} (O1-C7-C8-C6)16
646	625	β (O1-C6-C8)13
595	576	β (C10-N5-C7)11
530	513	τ(H21-O1-C6-C7)82
505	489	β_{out} (O3-C9-C10)14 + β (O4-C11-C7)19
477	462	β (O4-C11-C7)15 + β (C6-C7N5)16
332	321	τ_{out} (H24-O4-C11-C7)89

3.3.2. C-H vibrations

In the region of 3100-3000cm^{-1}, which is the characteristic region for the detection of C-H stretching vibration [34], the hetero aromatic structure demonstrates the existence of C-H stretching vibration. Theoretically, CH stretching modes are assigned at 3005, 2964, 2927 and 2922cm^{-1}. The vibration involving CH in and out of plane bending is found 1462 and 1442 cm^{-1} which agrees well with the FTIR spectrum of Migalastat.

3.3.3. C-N and C-O vibrations

C-O vibrations are found at 1038, 1012 and 969 cm^{-1}, which are good agreement with the bands in FTIR spectra of Migalastat.

Because of the possibility of mixing with other vibrations, the recognition of stretching of C-N is not a simple task. As anticipated, the stretching of C-N for Migalastatis noticed at 1109, 1088, and 790 cm^{-1}.

3.3.4. C-C vibration and N-H vibration

The ring C-C stretching vibration in Migalastat is calculated at 1412, 1343 and 1284cm^{-1} and N-H vibration occurs at 3382 cm^{-1} with 100% contribution to P.E.D.

3.4. Electric moment

The various properties of Migalastat, such as polarizability, first order hyperpolarizability and dipole moment were computed using the DFT/B3LYP/6-311G(d,p) approach and are listed in Table 4. "The dipole moment in a molecule is an important feature that is mostly used to study the intermolecular interactions involving the non-bonded type dipole-dipole interactions, because higher the dipole moment, stronger will be the intermolecular interactions". In the case of Migalastat, the predicted dipole moment is found to be 1.5943 D. The much lower FMO gap and significant dipole moment reflect its enhanced bioactivity and lessened stability. The calculation of polarizability (α) and first hyperpolarizability (β_{total}) is based on the finite field approach. The β_{total} is a tensor of third rank that can be expressed by a 3 ×3 ×3 matrix. Because of Kleinman symmetry [35], the 27 components of the matrix can be diminished to 10 components. Theoretically computed value of α and β_{total} for Migalastat are 0.1290×10^{-24}esu and 0.9487×10^{-30} esu respectively. The purpose of this computation is to learn more about the properties of NLOs. Urea is one of the model molecule having β_{total}value (0.1947×10^{-30}e.s.u), chosen for comparison. The computed value of for the title chemical is five times that of urea, indicating that the Migalastat has significant NLO characteristics.

Table 3: Computed ground state parameters of Migalastat

Parameters	Value
Energy	-592.2489 a.u.
HOMO-LUMO energy gap	6.827eV
Dipole moment	1.5943 Debye

Table 4: Computed value of components of electric moment of Migalastat

Dipole Moment(μ_{total}) in Debye		First order static hyperpolarizability (β)	
μ_x	-1.2406	β_{xxx}	-7.6899388
μ_y	-0.2533	β_{xxy}	-62.2076477
μ_z	-0.9687	β_{xyy}	-7.7925095
μ_{tot}	1.5943	β_{yyy}	17.9571298
Polarizability (α_o) in esu.		β_{xxz}	2.7722112
α_{xx}	96.4363173	β_{xyz}	14.552636
α_{xy}	1.328133	β_{yyz}	-31.4316408
α_{yy}	86.1270845	β_{xzz}	10.8984821
α_{xz}	-1.4465631	β_{yzz}	-7.8808732
α_{yz}	-2.3388947	β_{zzz}	-67.8820106
α_{zz}	78.5869839	β_{total} (au)	109.8132
α_o(esu)	0.1290×10^{-24}	**β_{total} (esu)**	0.9487×10^{-30}

3.5. Global Reactivity and thermodynamic parameters

Chemical potential, electronegativity, hardness, softness, and electrophilicity index are all global reactivity descriptors that are frequently established during the DFT stage. The electronic chemical potential, which describes the escape propensity of electrons from a stable system, is commonly computed

as μ=- (IP + EA)/2, according to Parr and Pearson [36]. Negative electronic chemical potential is described as electronegativity (χ). Chemical hardness, defined as (IP- EA)/2, is a measure of a chemical system's resistance to changes in electron distribution and is linked to its stability and reactivity. The global softness S = 1/η represents the reciprocal of the hardness. Parr et al. [36] established the global electrophilicity index (ω), which is derived as $\omega = \mu^2/2\eta$ in terms of chemical potential and hardness. Table 5 shows the global reactivity parameters for Migalastat.

In Table 5, various thermodynamic parameters for the title chemical are analyzed and given, including zero point energy (ZPE), thermal energy at room temperature (E), thermal enthalpy, thermal free energy, heat capacity (Cv), and entropy (S). These characteristics can be highly useful in predicting molecular reaction routes.

Table 5: Global Reactivity and Thermodynamic parameters for Migalastat

Global Parameters (eV)	Formula	Numerical values	Thermodynamic Parameters	Values
Ionization Potential	$IP= -E_{HOMO}$	6.205	Electronic energy (Hartree)	-592.2489
Electron affinity	$EA= -E_{LUMO}$	-0.622	ZPE (kcal/mol)	128.614
Electronic chemical potential	μ= -(IP+EA)/2	-2.791	Thermal energy (kcal/mol)	135.982
Electronegativity	χ =(IP+EA)/2	2.791	Thermal enthalpy (kcal/mol)	136.572
Chemical hardness	η = (IP-EA)/2	3.413	Thermal free energy (kcal/mol)	105.521
Global softness	S = 1/η	0.292	Constant volume heat capacity (cal/mol-K)	44.503
Global electrophilicity index	ω = χ2 /2 η	1.141	Entropy (cal/mol-K)	104.147

3.6. Local reactivity descriptors

NBO population methods were utilized to generate condensed Fukui functions (f_k), one of the most commonly used local reactivity descriptor.

Table 6: Local reactivity descriptors for Migalastat

ATOM	f_k^+	f_k^-	f_k°
O1	0.39453	-0.37521	0.00966
O2	0.40972	-0.37444	0.01764
O3	0.4563	-0.36805	0.044125
O4	0.36784	-0.36147	0.003185
N5	**0.83679**	-0.33077	**0.25301**
C6	-0.00565	0.04475	0.01955
C7	0.01253	-0.02801	-0.00774
C8	-0.06246	0.04856	-0.00695
C9	0.02291	0.05364	0.038275
C10	0.10407	-0.10686	-0.0014
C11	0.00207	-0.01155	-0.00474
H12	-0.05517	0.08572	0.015275
H13	-0.0496	0.08383	0.017115
H14	-0.08264	0.08425	0.000805
H15	-0.06788	0.0862	0.00916
H16	-0.0658	0.09987	0.017035
H17	-0.04907	0.0955	0.023215
H18	-0.15222	0.17909	0.013435
H19	-0.07432	0.09159	0.008635
H20	-0.09291	0.10201	0.00455
H21	-0.22037	**0.23549**	0.00756
H22	-0.21856	0.22222	0.00183
H23	-0.20758	0.22734	0.00988
H24	-0.20254	0.21631	0.006885

The equations that regulate nucleophilic, electrophilic, and radical attacks are as follows $f_k^+ = [q_k(n+1) - q_k(n)]$, $f_k^- = [q_k(n) - q_k(n-1)]$ and $f_k^0 = [q_k(n+1) - q_k(n-1)]/2$ respectively [37]. NBO population analysis at the B3LYP/6-311G (d,p) was used to calculate the natural atomic charges.

Fig.5 provides a visual representation of the computed Fukui functions (Table 6). As seen from the Table 6, the reactivity order for nucleophilic attack is N5>O3> O2>O1>O4. The reactivity order of the preferred atomic site for electrophilic attack is H21>H23>H22> H24>H18 while the sites for the free radical attack are in the order of N5>O3>C9>H17>C6.

3.7. NBO Evaluation

The natural bond orbital evaluation provides the precise doable natural Lewis structural image. It explains properly the interaction between each crammed and virtual orbital areas. The NBO evaluation explains the conjugative interaction in a very molecular system. A stabilizing donor acceptor interaction takes place when density of electron delocalizes between occupied Lewis type (bond or lone pair) NBO orbital and unoccupied (antibond or Rydgberg) non-Lewis NBO orbital. The NBO evaluation of the title chemical at the same level of theory has been undertaken to explain charge transfers, intra-molecule re-hybridi-zation, and delocalization. The investigation of the Fock matrix in the NBO basis of the molecule using second

order perturbation theory reveals substantial intramolecular hyper conjugative interactions, as seen in Table 7. From Table 7, it is clear that the strongest intramolecular hyperconjugative interaction occurs due to superimposition of lone pair of O1 over σ* (C6-H12) having stabilization energy of 8.43 kcal/mol. The second strongest intra molecular hyperconjugative interaction occurs between lone pair of N5 with antibonding orbitals σ*(C6-C7) and σ*(C9-C10) having interaction energy 8.12 kcal/mol. Another significant interaction are lone pair of O3 with σ*(C9-C10) and σ*(C9-H15) (interaction energies 7.45and 3.94 Kcal /mol respectively). There are also an interaction between overlapping of lonepair of O4 over antibonding σ*(C7-C11) and σ*(C11-H19) having energy 6.60 and 4.77 Kcal/mol respectively. Bonding orbital σ (C7-H13) interacts with antibonding orbitals σ*(O1-C6) and σ*(N5-H18) with interaction energies 3.99 and 3.21 Kcal/mol respectively.

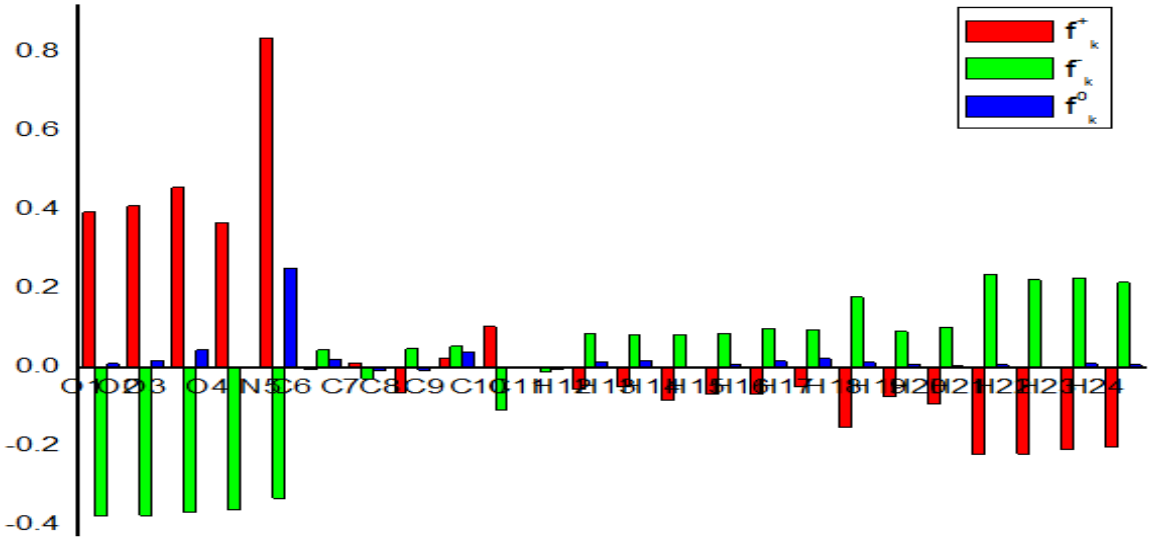

Fig. 5: Graphical view of Fukui function considering NBO charges

Table 7: NBO assessment of title compound

Donor NBO (*i*)	occupancy (*i*)	Acceptor NBO (*j*)	occupancy (*j*)	$E^{(2)}$ (kcal/mol	(*Ej–Ei*) a.u	*F*(*i*,*j*) a.u.
σ (C6-H12)	1.97589	σ*(N5-C7)	0.02432	3.94	0.86	0.052
σ (C6-H12)	1.97589	σ*(C8-C9)	0.03842	3.07	0.87	0.046
σ (C7-H13)	1.96714	σ*(O1-C6)	0.02514	3.99	0.79	0.050
σ (C7-H13)	1.96714	σ*(N5-H18)	0.01919	3.21	0.92	0.049
σ (C8-H14)	1.97409	σ*(O1-C6)	0.02514	3.59	0.80	0.048
σ (C10-H16)	1.98007	σ*(N5-C7)	0.02432	3.76	0.86	0.051
σ (C10-H17)	1.98028	σ*(N5-H18)	0.01919	3.06	0.92	0.047
σ (C11-H19)	1.98657	σ*(C6-C7)	0.04838	3.49	0.88	0.050
LP(2)O1	1.95382	σ*(C6-C8)	0.04424	3.81	0.66	0.045
LP(2)O1	1.95382	σ*(C6-H12)	0.03627	8.43	0.71	0.069
LP(2)O2	1.95143	σ*(C6-C8)	0.04424	6.21	0.68	0.058
LP(2)O3	1.95558	σ*(C9-C10)	0.04615	7.45	0.67	0.063
LP(2)O3	1.95558	σ*(C9-H15)	0.03265	3.94	0.71	0.047
LP(2)O4	1.95591	σ*(C7-C11)	0.03443	6.60	0.68	0.060
LP(2)O4	1.95591	σ*(C11-H19)	0.02423	4.77	0.70	0.052
LP(1)N5	1.91590	σ*(C6-C7)	0.04838	8.12	0.67	0.066
LP(1)N5	1.91590	σ*(C9-C10)	0.04615	8.12	0.66	0.066

4. CONCLUSION

Quantum chemical study on Migalastat was analyzed at DFT level employing the 6-311G(d,p) basis set. Theoretical vibrational analysis has been done and all the assignments are well matched with standard one. HOMO-LUMO band gap of the title molecule is found to be 6.827eV, which explains its chemical reactivity and is also accompanied by chemical hardness.The MESP analysis of the molecule under study was successfully used to describe its characteristics. β_{total}value of molecule under study are found to be 0.9487×10^{-30}e.s.u approximately 5 times greater than value of urea revel its significant behavior toward nonlinear property. Various global reactivity descriptors and thermodynamic parameter was also calculated which gives its reactivity and reaction paths of the Miglastat. The reactivity order of the chosen atomic sites using the fukui function was also determined and its order for nucleophilic attack is N5>O3>O2>O1>O4, electrophilic attack is H21>H23>H22>H24>H18 and for the free radical attack is N5>O3>C9>H17>C6. A strong intra molecular interaction occur between lone pair of N5 with antibonding σ*(C6-C7) and σ*(C9-C10) having stabilization energy 8.12 kcal/mol were observed with its full NBO analysis. The higher value of total hyperpolarizibility shows that the title molecule possibly has good NLO agent. We hope that our research opens up new avenues for researchers to pursue additional research on the title chemical.

Conflict of interest

The authors state that they have no known competing financial interests or personal relationships that could appear to influence the work reported in this paper.

Source of funding

None declared

5. REFERENCES

1. Drugs to fix "misfolded" proteins could cure a range of diseases": Gizmag.com. Retrieved 2013; 12-10.
2. Martina Gaggl, Gere Sunder Plassmannx. *Nature Reviews Nephrology*, 2016; **12**:653-654.
3. Hoffmann B, Schwarz M, Mehta A, Keshav S. *Clin Gastroenteral Hepatol.,* 2007; **5(12)**:1447-1453.
4. Gold KF, Pastores GM, Botteman MF, et al. *Qual Life Res.*, 2002; **11(4)**:317-327.
5. Benjamin ER, Della Valle MC, Wu X, et al. *Genet Med.,* 2017; **19(4)**:430-438.
6. Galafold [summary of product characteristics], Buckinghamshire, UK, Amicus Therapeutics UK Ltd, http://www.ema.europa.eu/docs/en_GB/document_library/EPAR_Product_Information/human/004059/WC500208434.pdf,2017
7. P. R. Griffiths in Handbook of Vibrational Spectroscopy, Eds. Chalmers J. M. and Griffiths P. R, *John Wiley &Sons, Inc., New York*, 2002.
8. Stuart B. Biological applications of Infrared Spectroscopy, *John Wiley and Sons*, *New York*, 2008.
9. Barth A, Zscherp C. *Reviews of Biophysics*, 2002; **35**:369-430.
10. Dinorah G, Lucia O, Vieites M, Boiani M, Gonzalez M, Baran E J, Cerecetto H. *Spectrochim. Acta Part A: Mol. Biomol. Spectrosc.*, 2007;**68**;341-348.
11. Ali HRH, Edwards HGM, Kendrick J, Scowen IJ. *Spectrochim. Acta A: Mol. Biomol. Spectrosc.*, 2009; 715-719.
12. Frisch MJ, Trucks GW, Schlegel HB, Scuseria GE, Robb MA, Cheeseman JR, et al. *Gaussian 03 Revision C.02*, *Gaussian Inc.*, Pittsburgh, PA, 2003.
13. Schlegel HB. *J. Comput. Chem.,* 1982; **3:**214.
14. Lee C, Yang W, Parr RG. *Phys. Rev. B,* 1988*;* **37:**785.
15. Jones RO, Gunnarson O. *Rev. Mol. Physics,* 1989; **61:** 689.
16. Kohn W, Sham L J. *Phys. Rev. A,* 1965; **140:**1133.
17. Frisch A, Nelson A B, Holder A J, *GAUSSVIEW Inc.*, Pittsburgh PA, 2000.
18. Scott A P, Random L. *J. Phys. Chem., 1996;* **100**: 16502-16513.
19. Pulay P, Fogarasi G, Pongor G, Boggs JE, Vargha A. *J. Am. Chem. Soc.*, 1983; **105**:7037-7047.
20. Jamroz H. Vibrational Energy Distribution Analysis: VEDA 4 Program, Warsaw, Poland, 2004.
21. Buckingham AD. *Adv. Chem. Phys.,* 1967; **12**:107-142.
22. Kanis DR, Ratner MA, Marks TJ. *Chem. Rev.*, 1994; **94**:195-242.
23. Kumar A, Narayan V, Prasad O, Sinha L. *J. Mol. Struct.*, 2012; **1022**:81-88.
24. Ggadre SR, Pathak RK. *J. Chem. Phys.*, 1990; **93**:1770-1774.
25. Ggadre SR, Shrivastava IH. *J.Chem. Phys.*, 1991; **94**:4384-4390.

26. Murray JS, Sen K. Molecular Electrostatic Potentials, Concepts and Applications, *Elsevier*, Amsterdam, 1996.
27. Alkorta I, Perez JJ. *Int. J. Quant. Chem.,* 1996; **57:** 123–135.
28. Scrocco E, Tomasi J. *Advances in Quantum Chemistry*, 1978; Vol. 2, P. Lowdin, ed.: Academic Press, New York.
29. Luque FJ, Orozco M, Bhadane PK, Gadre SR. *J. Phys. Chem.*,1993; **97**:9380-9384.
30. Sponer J, Hobza P. *Int. J. Quant. Chem.,* 1996; **57**:959-970.
31. Pulay P, Fogarasi G, Pongor G, Boggs JE, Vargha A. *J. Am. Chem. Soc.*,1983; **105**:7037-7047.
32. Scott A P, Random L. *J. Phys. Chem. US*, 1996; **100**:16502-16513.
33. Jag M. Organic Spectroscopy - Principles and Applications. **2nd ed**.: Narosa Publishing House, New Delhi; 2001.
34. Yadav KK, Kumar A, Kumar A, Misra N, Brahmachari G. *Journal of Molecular Structur*e, 2018; **115**3:1-10.
35. Kleinman DA. *Phys. Rev.*, 1962; **126:**1977-1979.
36. Parr RG, Pearson RG. *J. Am. Chem. Soc.*, 1983; **105:**7512-7516.
37. Ayers PW, Levy M. *Theor. Chem. Acc.,* 2000*;* **103**:353-360.